

Spin-flip Raman scattering in CdTe/Cd_{1-x}Mn_xTe multiple quantum wells: A model system for the study of electron-donor binding in semiconductor heterostructures

M. P. Halsall, S. V. Railson, D. Wolverson, and J. J. Davies
School of Physics, University of East Anglia, Norwich NR4 7TJ, United Kingdom

B. Lunn and D. E. Ashenford
Department of Engineering Design and Manufacture, University of Hull, Hull HU6 7RX, United Kingdom
(Received 18 March 1994; revised manuscript received 27 June 1994)

The spin-flip Raman scattering of electrons bound to donors in CdTe/Cd_{1-x}Mn_xTe multiple-quantum-well structures at 1.6 K in magnetic fields up to 6 T has been studied for a range of samples forming two series in which, first, the CdTe quantum-well width and second, the Cd_{1-x}Mn_xTe barrier composition x were varied systematically. For structures with $x < 0.1$, two spin-flip Raman bands are observed, which can be assigned to electrons located in the quantum wells and bound to donors located either in the quantum wells themselves or in the barriers of the structure. Measurements of the excitation spectra of the two Raman bands and of the quantum-well photoluminescence support this assignment. A variational calculation allows us to simulate the form of the observed spectra and also gives a quantitative description of the dependence of the Raman peak positions on the well width and barrier composition. The calculation allows us to derive a value of 0.060 ± 0.005 eV for the conduction-band offset when $x = 0.07$.

I. INTRODUCTION

Dilute magnetic semiconductors (DMS) such as Cd_{1-x}Mn_xTe are of special interest because of the large exchange interactions between the charge carriers and the magnetic ions.¹ As a result of this interaction, the magnetic properties of the electrons and holes are considerably enhanced and at low temperatures it becomes possible to produce significant changes in the energy positions of the band edges simply by applying an external magnetic field. This band-edge tunability assumes special importance when DMS alloys are incorporated into multiple-quantum-well (MQW) structures, since it can be used to vary the band offsets in a given specimen and thus to investigate aspects of quantum-well behavior in a way that is impossible in conventional semiconductor materials. The most studied of DMS heterostructure systems is CdTe/Cd_{1-x}Mn_xTe and several photoluminescence (PL) and photoluminescence-excitation (PLE) spectroscopy investigations have been reported,²⁻⁷ with special emphasis attached to the determination of band offset ratios and to the behavior of exciton energies in confined layers in the presence of magnetic fields. Considerable insight into the magnetic properties of bulk Cd_{1-x}Mn_xTe has also been gained from spin-flip Raman (SFR) scattering experiments⁸⁻¹¹ and a number of such studies have also been made of MQW structures based on Cd_{1-x}Mn_xTe.¹²⁻¹⁴

In the present study, we have concentrated on the properties of electrons that interact with donors in CdTe/Cd_{1-x}Mn_xTe MQW structures. We have used magnetic fields to vary the heights of the conduction band barriers presented by the Cd_{1-x}Mn_xTe layers and spin-flip Raman spectroscopy to investigate the consequent changes in the energies of the electrons in the CdTe

wells. In these systems, the depth of the electron potential well depends markedly on the spin state (Fig. 1), so that the energy levels of the electrons in the well are split into two, in a manner that depends sensitively on the magnetic fields and on the conduction-band offset, Δ_c . It is this energy splitting, δE_w , that is measured directly in the SFR experiment.

In a uniformly-doped n -type structure with *wide* quantum wells, the electrons in the well regions will consist of two types. First, there will be those bound at the donors in the wells themselves and, secondly, there will be those which originated from the donors in the barriers, but which are now trapped in the well region. As the well width is decreased, the effect of the well potential on the wave functions of the neutral donors in the wells will be-

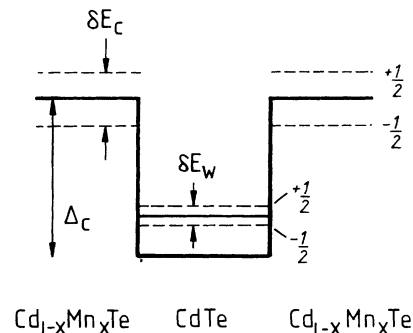


FIG. 1. Schematic diagram of a CdTe quantum well between Cd_{1-x}Mn_xTe barriers. Δ_c is the conduction-band offset; δE_c and δE_w are the splittings in energy of the barrier and well electron states with $m_j = +1/2$ and $m_j = -1/2$ in an applied magnetic field.

come increasingly important. At the same time, the influence of the Coulomb field of the ionized donors in the barriers on the electrons that they have lost to the wells will become significant. In the Raman experiment to be described, we have been able to distinguish between these two types of electrons and thus to study the interaction between electrons in the well regions and ionized donors in the barriers. This has been made possible by the use of low manganese concentration in the barriers, so that the conduction-band offsets are sufficiently small for the Coulomb field of the ionized donors in the barriers to affect strongly the behavior of the electrons in the wells. The SFR signals associated with the two types of electron are then distinct.

Brief accounts of some of the present results have been given already.¹⁵⁻¹⁶ In the present paper, we give further experimental data (including data on the resonance effects of the Raman signals) and discuss in more detail the theoretical model and the differences between our results and those reported for similar systems. We are also to deduce a value for the conduction-band offset and hence find (for $x = 0.07$) that the valence-band offset for CdTe/Cd_{1-x}Mn_xTe is larger than proposed in some of the earlier studies of these materials.

II. EXPERIMENTAL DETAILS

The specimens were grown by molecular-beam epitaxy at about 240°C on 1000 Å buffer layers of CdTe on (001) substrates of InSb.¹⁵ The MQW structures each consisted of 15 CdTe layers between the Cd_{1-x}Mn_xTe barriers, there being no capping layer. Two series of specimens were studied, all with barrier widths of 150 Å. In the first series, the manganese concentration in the barriers was in the region of 0.07, with CdTe well widths ranging from 50 to 85 Å. In the second series, the well width was kept constant at 50 Å while the manganese concentration x in the barriers was varied between 0.01 and 0.12. The relevant details are given in Table I. The well thicknesses were checked by x-ray double crystal rocking curve measurements, which showed that the structures were of high quality with good uniformity of period, while the barrier concentrations were confirmed via photoluminescence spectra and photoluminescence excitation spectroscopy. A thick epitaxial layer of Cd_{0.93}Mn_{0.07}Te was also studied in order to check the manganese magnetization under the conditions of our experiments. Further details of the growth procedure are given elsewhere.^{4,6} Though not intentionally doped, the material grown is typically n -type, with net (i.e., uncompensated) neutral donor concentrations at low temperature of order 10^{14} cm⁻³, as determined by capacitance-voltage measurements in thick layers.

The Raman experiments were carried out with the specimens immersed directly in superfluid helium at about 1.6 K inside a superconducting split-coil magnet in magnetic fields up to 6 T. A titanium-sapphire laser pumped by an argon-ion laser was used as the tunable excitation source, care being taken to keep the power sufficiently low for there to be no dependence of the Raman shifts on excitation density (as can occur if there are

TABLE I. Sample parameters. Each specimen has 15 quantum wells, with the exception of *M394*, which is a single layer.

Specimen number	CdTe well width (Å)	Cd _{1-x} Mn _x Te barrier width (Å)	Barrier manganese concentration
First series			
<i>M395</i>	35	150	0.07
<i>M360</i>	50	150	0.07
<i>M296</i>	75	150	0.07
<i>M362</i>	85	150	0.07
Second series			
<i>M468</i>	50	150	0.01
<i>M469</i>	50	150	0.02
<i>M470</i>	50	150	0.03
(<i>M360</i>)	50	150	0.07
<i>M484</i>	50	150	0.12
Other samples			
<i>M394</i>	none	thick epilayer	0.066
<i>M387</i>	15	150	0.094
<i>M213</i>	75	75	0.24

sample heating effects). The scattered light was analyzed with an Instruments SA (Jobin-Yvon) triple monochromator using an Astromed charge-coupled-device array detector. The dependences of the Raman signal intensities on the wavelength of the laser (the Raman resonance profiles) were measured with an automated scanning technique that has been described elsewhere.¹⁷ Photoluminescence excitation spectra were determined by monitoring the PL intensity as the excitation laser was stepped in fixed wavelength intervals; correction was made for any small variations in incident laser power. Care was taken to determine Raman resonance profiles and PLE spectra for the same region of the specimen, and using the same experimental conditions.

The Raman spectra were taken in the backscattering geometry, with the light being incident in the [001] direction (Z) perpendicular to the magnetic field, which was in the plane (XY) of the epitaxial layers (the spectra reported here are thus for normal incidence and differ from those in Ref. 15 which were for light incident on the specimen at 45°). As demonstrated in Sec. IV, the Raman scattering is very strongly enhanced when the incoming or outgoing photon energies are in resonance with the energy of what is presumed to be an excitonic transition. The spin flip of an electron in a scattering process requires that the angular momentum of the outgoing photon differs by unity from that of the incoming one. The selection rules are satisfied if the incoming light is σ polarized, the scattered light being π polarized. In terms of the Damen, Porto, and Tell¹⁸ notation, this is written $Z(\sigma, \pi)\bar{Z}$, where the symbols outside the brackets refer to the directions of incidence and observation and where (σ, π) denotes the sense of polarization of the electric-field vector [the inverse process $Z(\pi, \sigma)\bar{Z}$ would also be allowed by the selection rules].

III. THE RAMAN SPECTRA

We begin with the spin-flip scattering for specimens with $x = 0.07$ in the barriers. An unusual feature of the spectra from each of these specimens is the occurrence of *two* distinct peaks, which we denote by SF1 and SF2 [for example, for a well width L_w of 50 Å, signals occur at 38 cm⁻¹ (SF1) and 51 cm⁻¹ (SF2) at a field of 6 T at 1.6 K].

As the magnetic field is increased from zero, the Raman shifts corresponding to SF1 and SF2 increase as shown in Figs. 2(a) and 2(b) (for the specimen with $x = 0.07$ and $L_w = 50$ Å, number M360). The behavior is characteristic of SFR signals from samples containing DMS material,⁸ in which the exchange field follows the manganese magnetization and eventually saturates. It is well established that in bulk Cd_{1-x}Mn_xTe the conduction band splits under the action of a magnetic field according to¹

$$\delta E_c = -xN_0\alpha\langle S_z \rangle^{\text{Mn}} + g_e\mu_B B, \quad (1)$$

where g_e is the electron magnetogyric ratio, μ_B is the Bohr magneton, $\langle S_z \rangle^{\text{Mn}}$ is the thermal average of the Mn²⁺ spin projection in the field direction, α is the exchange constant for the conduction band (normalized to the unit cell volume), and N_0 is the number of cations per unit cell.

At the temperatures and manganese concentrations used in the current experiments, the Cd_{1-x}Mn_xTe is in

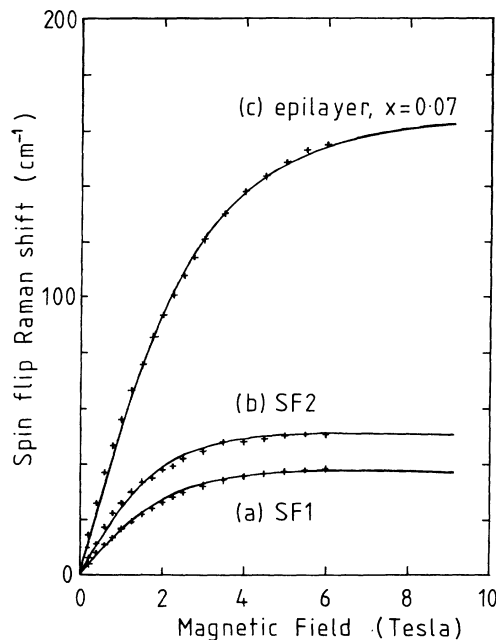


FIG. 2. The spin-flip Raman (SFR) shift as a function of the applied magnetic field for a multiple-quantum-well sample (M296) with a well width of 75 Å and a barrier Mn concentration of 0.07 at nominal temperature 1.6 K, for (a) the SF1 and (b) the SF2 signals. For comparison, (c) shows the SFR shift observed in an epilayer of Cd_{0.93}Mn_{0.07}Te, sample M394. The points are experimental data and the curves are fits using the modified Brillouin function (as described in the text) and a normal conduction-band Zeeman term.

the paramagnetic state.¹ It is well known, however, that the effective magnetization is reduced relative to that expected for an assembly of noninteracting Mn²⁺ ions because of the tendency for those ions that are nearest neighbors to align antiferromagnetically. This can be modeled satisfactorily¹ by replacing x by an effective concentration \bar{x} (where \bar{x} is less than x) and by using a Brillouin function $B_{5/2}(y)$ in which the argument is modified to $y = Sg_{\text{Mn}}\mu_B B / k_B T_{\text{eff}}$, where $S = \frac{5}{2}$, g_{Mn} is the Mn²⁺ magnetogyric ratio, k_B is the Boltzmann constant, and $T_{\text{eff}} = (T + T_0)$ is an effective temperature. Values of the magnetization splitting and of T_0 for different concentrations x have been measured for epitaxial material by various groups,¹⁹⁻²¹ whose data agree well for $x < 0.10$ and indicate that, for $x = 0.07$, the value of \bar{x} is about 0.04 and T_0 is about 2.2 K. At low temperatures and moderately high fields, the magnetization of the Mn²⁺ spin system approaches saturation ($\langle S_z \rangle$ tends to $-\frac{5}{2}$) and the value of the Cd_{1-x}Mn_xTe band splitting is now given by

$$\delta E_c = \frac{5}{2}\bar{x}N_0\alpha + g_e\mu_B B. \quad (2)$$

For values of x of about 0.07, the saturation condition is approached at 1.6 K at about 6 T.

The electron energy level in the well splits by an amount $g_e\mu_B B$ due to the standard Zeeman interaction (we take g_e to have the same value in the well and in the barrier) plus an amount which is proportional to δE_c (provided that δE_c is not too large compared with the band offset Δ_c). The electron spin-flip energy should thus be the sum of a term linear in field ($g_e\mu_B B$) and a term that follows the form of the modified Brillouin function $B_{5/2}(y)$. The size of the second term depends on the ratio of δE_c to Δ_c (it is in essence a measure of the electron penetration into the barrier) and is thus sensitive to the band offset.

To fit the data we use the value $g_e = -1.59$ measured for CdTe.²² In Fig. 2(c) we show the results for electron spin-flip scattering for a "bulk" layer of the same concentration as the barriers. The splitting for the bulk layer allows us to obtain the quantity $(\frac{5}{2}\bar{x}N_0\alpha)$ without having to measure the concentration x . The value obtained (165 cm⁻¹) is, however, consistent with $x = 0.07$. We find that the values of T_0 found for the SFR energies of electrons in the wells are slightly lower than those that are reported for bulk materials of the same manganese concentration as the barriers.¹⁰

The observation of *two* SRF signals (SF1 and SF2) associated with the well region is the distinct feature of our spectra: we shall show later that they are due, respectively, to electrons bound at neutral donors in the wells and to electrons that are present in the wells as a result of the ionization of donors in the barriers. We shall show that these two types of electron do indeed lead to different SFR energies, thus accounting for the existence of the two signals.

Before proceeding, we must ask whether or not one should expect to observe SFR from specimens containing only 10¹⁴ neutral donors per cm⁻³. We note that Gu-

barev, Ruf, and Cardona,¹¹ in a study of *p*-doped $\text{Cd}_{0.95}\text{Mn}_{0.05}\text{Te}$ with an effective donor concentration of $5 \times 10^{16} \text{ cm}^{-3}$, observed SFR from *photoexcited* electrons at laser powers of about 1 mW. If it is assumed that all incident photons are absorbed in a volume of 1 mm^2 by $1 \mu\text{m}$ in their experiment and that each creates one electron, the excited carrier density would be of order $10^{21} \tau_d$, where τ_d is the recombination time in seconds. Since this figure is an upper limit and since τ_d is likely to be less than 1 ns, the fact that we can observe electron SFR at neutral donor concentrations of 10^{14} cm^{-3} is entirely reasonable. The strong resonant enhancement is essential to such observations and we therefore investigated this in some detail.

IV. THE RESONANCE BEHAVIOR OF THE RAMAN SIGNALS

The intensities of the Raman spectra from all specimens show a very strong dependence on the laser wavelength, as has been observed previously.¹¹ This is demonstrated in Fig. 3, where a set of Raman spectra recorded at different laser energies are shown. In each case, the *x* axis of the spectrum covers the same Raman shift range ($10\text{--}80 \text{ cm}^{-1}$ relative to the laser position). Successive spectra were recorded for laser wavelengths at 0.1 nm intervals and were then plotted displaced along the *z* axis. In this figure, Raman signals can be identified easily since they appear at a constant Raman shift from the laser energy, and thus at a constant position along the *x* axis, whereas PL signals would move diagonally, being at a constant absolute energy.

The dramatic resonant enhancement of the SF1 and SF2 signals is clear from Fig. 3, but still more may be

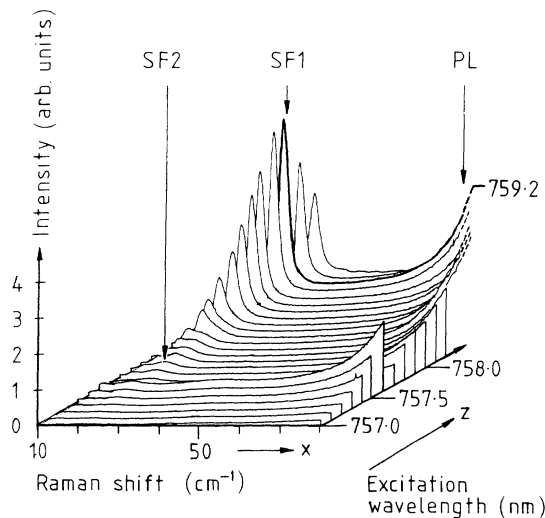


FIG. 3. The spin-flip Raman signals (SF1 and SF2) of a multiple-quantum-well sample (*M296*) with a well width of 75 \AA and a barrier Mn concentration of 0.07 at 1.6 K in a magnetic field of 4 T. Each spectrum covers the range of Raman shifts from 10 to 80 cm^{-1} from the laser line, and successive spectra were recorded with the laser at 0.1-nm wavelength intervals. The back, right-hand corner of this diagram would be obscured by a very strong PL signal and has been omitted here.

learnt by extracting from these data the resonance profiles of the signals. Since the SF1 and SF2 bands overlap, two-Gaussian fits were again used to determine their separate integrated intensities,¹⁶ which were then plotted as a function of laser energy in Fig. 4(b). Also shown in Fig. 4(a) in the PLE spectrum for the dominant emission line of the same sample in the same experimental geometry as for the SFR measurements. The interpretation of the PLE in detail lies beyond the scope of the present paper, but the maxima may be assumed to correspond to the energies of free-exciton transitions in the quantum well, since these have a high density of states, whereas the maxima of the resonance profiles of SFR signals arising from electrons bound to donors should correspond to the energies of donor-bound exciton states. By carrying out measurements at different magnetic fields, we have shown that the shift (marked Δ) between the SF1 resonance and the second PLE peak is constant and therefore that these two features are associated with the same excitonic spin state. The existence of the shift Δ is consistent with our model for the origin of the SFR signals and the magnitude of Δ (about 2 meV for the SF1 resonance) gives us an estimate of the localization energy of the exciton at the donor. This point has been dis-

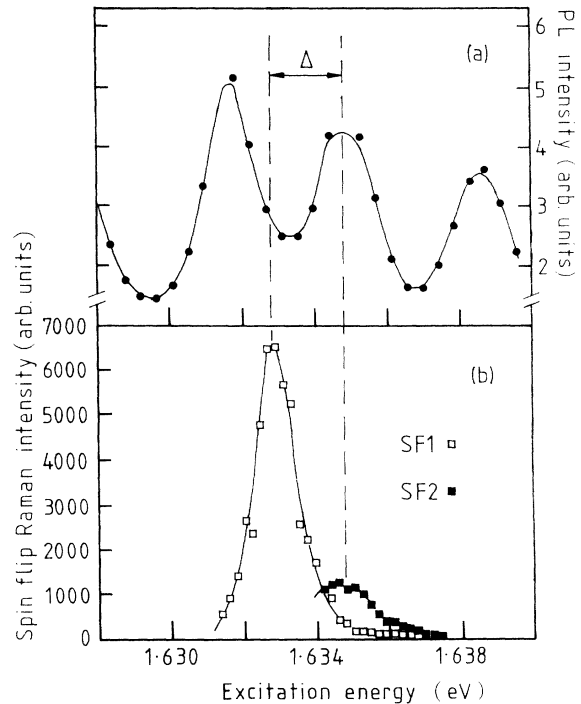


FIG. 4. (a) The photoluminescence excitation (PLE) spectrum of a multiple-quantum-well sample (*M296*) with a well width of 75 \AA and a barrier Mn concentration of 0.07 at 1.6 K in a magnetic field of 4 T. (b) The spin-flip Raman intensity (integrated over the fitted Gaussian line shapes of the SF1 and SF2 signals) as a function of the excitation laser energy for the same sample and conditions as (a); these data are derived from the spectra of Fig. 3. The symbols (\square , \blacksquare , \bullet) represent experimental data and the solid lines are guides to the eye.

cussed in more detail recently by Hirsch, Meyer, and Waag.²³

There remains the difference between the resonance energies of SF1 and SF2, as illustrated in Fig. 4. This difference is attributed to the difference in the positions of the donors responsible for the two signals SF1 and SF2, since the donor position affects the localization energy of the exciton at that particular donor, and therefore the resonance energy of the SRF signal associated with that donor. The observation of a higher resonance energy for SF2 than for SF1 supports our model for the origin of the SFR signals, since the exciton localization energy would be expected to decrease when the donor impurity is located in the barrier, leading to a resonance energy for SF2 closer to the transition energy of a free exciton.

V. INTERPRETATION OF THE SFR SPECTRA

In this section, we calculate the spin-flip energies expected for an electron subject to the combined effects of the well potential and of the Coulomb potential of the donor. We shall show that the result is sensitive to the position of the donor relative to the well center and that, under appropriate circumstances, a SFR spectrum is predicted with two distinct peaks, as observed experimentally in our range of specimens with $x \approx 0.07$. The peak separation is found to be sensitive to the value of the conduction-band offset and we exploit this fact to obtain an experimental measure of Δ_c .

We work within the effective-mass approximation, in which the Hamiltonian \mathcal{H} of an electron in the Coulomb field of a donor ion in a quantum well has the form²⁴

$$\mathcal{H} = \frac{\hbar^2}{2m_e^*} \left[\frac{1}{r} \frac{\partial}{\partial r} r \frac{\partial}{\partial r} + \frac{1}{r^2} \frac{\partial^2}{\partial \varphi^2} - \frac{\partial^2}{\partial z_e^2} \right] - \frac{e^2}{4\pi\epsilon_0\epsilon_r \sqrt{[r^2 + (z_e - z_d)^2]}} + V_e(z_e), \quad (3)$$

where m_e^* is the effective mass of the electron and $\epsilon_0\epsilon_r$ is the permittivity of the material.

In the cylindrical polar coordinates (r, ϕ, z) , the z direction is taken to be perpendicular to the layer planes. The quantities z_e and z_d define the positions along z of the electron and donor, respectively, while r defines the electron-donor separation in the layer plane. The origin of the z axis is taken to be zero at the center of the potential well, whose depth in zero field is Δ_c and whose width is $2a_w$. The electron potential is thus of the form (in zero field)

$$V_e(z_e) = \begin{cases} 0 & \text{for } |z_e| \leq a_w \\ \Delta_c & \text{for } |z_e| \geq a_w \end{cases}. \quad (4)$$

To obtain the electron energies we use a variational approach. Following Tanaka, Nagaoka, and Yamabe,²⁵ we assume a solution in factored form and use a trial wave function

$$\psi = f(z_e) e^{-b\sqrt{r^2 + z^2}}, \quad (5)$$

where b is a variational parameter, $z = (z_e - z_d)$, and

$f(z_e)$ is the appropriate finite quantum-well envelope wave function, thus,

$$f(z_e) = \begin{cases} \cos(k_e z_e) & \text{for } |z_e| \leq a_w \\ A_e \exp(-q_e |z_e|) & \text{for } |z_e| \geq a_w \end{cases}. \quad (6)$$

Here q_e , k_e , and A_e are obtained from the interfacial continuity condition on $f(z_e)$ and its derivative. The energy E_{var} is now calculated following the approach of Greene, Bajaj, and Phelps²⁶ and is minimized with respect to the variational parameter. The binding energy of the electron to the donor can be obtained by subtracting E_{var} from the finite well confinement energy in the absence of the donor, determined from the envelope function $f(z_e)$.

When a magnetic field is applied, the depth of the potential well seen by electrons of different spin alters, as described earlier. Thus, for the two spin states we can write

$$V_e(\pm \frac{1}{2}) = \begin{cases} \pm g_e \mu_B / 2 & \text{for } |z_e| \leq a_w \\ \Delta_c \pm \delta E_2 / 2 & \text{for } |z_e| \geq a_w \end{cases}, \quad (7)$$

where δE_c is given by Eq. (2) and includes the small electronic Zeeman term $g_e \mu_B B / 2$.

The variational calculation is now repeated for both directions of the electron spin and the difference gives the spin-flip energy at that particular magnetic field. We take the values $\epsilon_r = 9.4$ (Ref. 27) and $m_e^* = 0.096m_e$ (Ref. 28) for CdTe and, in the absence of other information assume the same values for Cd_{0.93}Mn_{0.07}Te (this also simplifies the interface continuity equations). In Fig. 5 we show the calculated binding energy E_d due to the donor as a function of donor position. For a donor in the center of the well, $|E_d|$ exceeds the hydrogenic three-dimensional bulk value of 14.8 meV (calculated using the values of m_e^* and ϵ_r given above), as expected. As the donor moves into the Cd_{0.93}Mn_{0.07}Te barrier, $|E_d|$ falls rapidly but even when the donor is at a distance of 100 Å from the interface, the binding energy is still 4 meV.

In comparing the spin-flip energies of the different structures we find it convenient to use the data taken at 6 T. At this field, the magnetization of the manganese spin system is almost saturated and Eq. (2) is valid. In Fig. 6 we show the calculated spin-flip energies at 6 T for all possible donor positions in M296 (75 Å CdTe wells, 150 Å Cd_{0.93}Mn_{0.07}Te barriers), the value of Δ_c being taken to be 0.06 eV.

The shape of the curve in Fig. 6 is the key to the understanding of our observed spectra, since it shows two turning values, at $z_d = 0$ and at z_d just inside the barrier. The observed spectrum will be the superposition of signals due to the differently located donors in the structure and hence, if a uniform spatial distribution of donors is assumed, there will be two peaks in the Raman spectra, corresponding to the turning values of Fig. 6. To make this clearer, we indicate at the edge of Fig. 6 how the SFR spectrum may be simulated by assuming the donors to be uniformly distributed in the wells and barriers on discrete sites of the zinc-blende crystal structure. First,

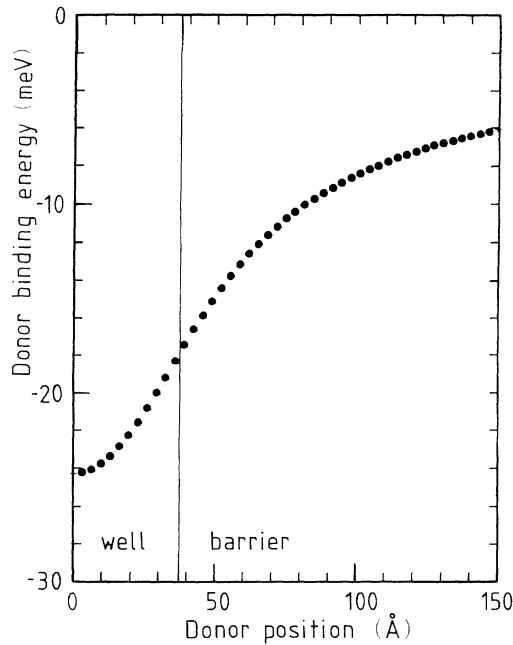


FIG. 5. The calculated binding energy of an electron to a donor as a function of the distance (along the growth axis) of the donor from the center of a quantum well of width 75 Å and a barrier Mn concentration of 0.07, in the absence of a magnetic field. The origin is chosen to be the center of the well and the vertical dashed line represents the position of the barrier/well interface. Successive points are one half of a lattice parameter apart.

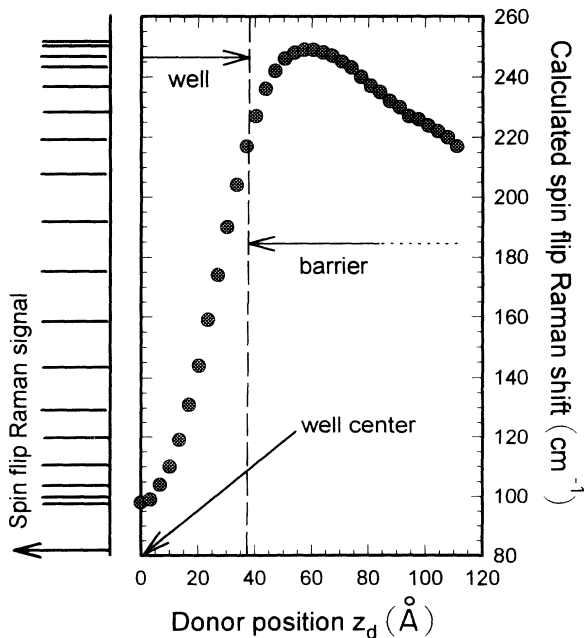


FIG. 6. The calculated spin-flip Raman shift of an electron bound to a donor, as a function of the position of the donor (measured from the center of the quantum well and along the growth axis) for a quantum well of width 75 Å and a barrier Mn concentration of 0.07 in an applied magnetic field (6 T) at which the barrier magnetization is saturated. The vertical dashed line indicates the position of the barrier/well interface. The “stick” diagram at the left shows how the calculated curve may be used to simulate the experimental spin-flip spectrum, as described in the text.

each donor within the range $z_d=0-60$ Å is assumed to give an identical contribution to the spectrum (as represented by the δ functions at the left of the diagram). Each δ function is then replaced by a Gaussian line shape of full width at half maximum of 1.6 cm^{-1} (the choice is not critical and the value chosen is typical of spin-flip signals from bulk material). The resulting composite spectrum then contains two peaks similar to those observed experimentally.

It should be noted that the different contributions to the spectrum (arising from different donor positions) have been assumed here to be equal in magnitude. The relative *intensities* of the two peaks of the experimental spectra are therefore not expected to be reproduced accurately, since the different resonance behavior of the SF1 and SF2 features (described in Sec. III) has not been accounted for. These resonance effects lead to a variation of the relative *intensities* of the SF1 and SF2 signals with laser wavelength, though fortunately the Raman *shifts* at the peaks are only weakly dependent on the excitation wavelength (a detailed discussion of these points will be presented elsewhere, though we note here that because excitons bound at donors with values of z_d beyond about 20 Å into the barrier are out of resonance with the laser in most of our experiments they have not been included as contributing to the composite spectrum at the edge of Fig. 6).

To test the model further we have calculated the energies of the SF1 and SF2 peaks as a function of well width for the specimens with barrier concentrations of $x=0.07$, assuming a conduction-band offset of $\Delta_c=0.06 \text{ eV}$. Allowance was made for the fact that the barrier magnetization has not quite saturated even at 6 T. The predicted shifts (Table II) agree excellently with those observed, both in their absolute values and in the differences between SF1 and SF2. The exception is *M395*, which has a thin well of only 35 Å and in which the effects of interdiffusion are believed to be important (see below).

One can define a parameter γ which represents the fraction of the total band offset that lies in the conduction band; the value of $\Delta_c=0.060 \text{ meV}$ corresponds to $\gamma=0.54$, given that the total band-gap difference between CdTe and $\text{Cd}_{1-x}\text{Mn}_x\text{Te}$ is $1.592x \text{ eV}^1$ at 2 K. The calculated spin-flip shifts are sensitive to the value assumed for the conduction band offset (in effect, the only adjustable parameter in the calculation). If γ is varied, the calculated Raman shifts become larger (because the penetration of the electron envelope wavefunction into the barrier increases): for example, for $\gamma=0.45$ ($\Delta_c=0.050 \text{ eV}$), all the saturation spin-flip shifts for the specimens with $x=0.07$ increase by about 4 cm^{-1} (compared with the experimental uncertainty of $\pm 2 \text{ cm}^{-1}$). To fit our observations, we thus find that Δ_c (strained) $=0.060 \pm 0.005 \text{ eV}$; for the CdTe/ $\text{Cd}_{1-0.93}\text{Mn}_{0.07}\text{Te}$ system, the strain contribution to Δ_c is about -3 meV , so that the “zero strain” value of the conduction-band offset is 0.063 eV (or, equivalently, $\gamma=0.57$). We discuss our result for γ more fully in Sec. VII.

In the same manner, we can predict the variation in spin-flip Raman shift for the “orthogonal” series of sam-

TABLE II. Spin-flip Raman shifts for different specimens at a magnetic field of 6 T and a temperature of 1.6 K. The calculated shifts make use of the data of Ref. 20 (in the second part of the table, the figures in parentheses makes use of the data of Ref. 21).

Sample parameters		Spin-flip Raman shift (cm ⁻¹)			
x	Well width (Å)	Observed (± 1 cm ⁻¹)	SF1 calculated	SF2 calculated	
0.07	50	38	51	37.6	50.5
0.07	75	18.5	29	18.0	28.4
0.07	85	14	21	13.2	21.0
0.01	50	18.5		17.2(16.4)	22.2(21.2)
0.02	50	40.2		30.0(28.0)	39.5(36.7)
0.03	50	36	46	35.2(34.2)	47.7(44.8)
0.07	50	38	51	41.0(37.1)	54.0(48.7)
0.12	50	40.2		34.2(31.3)	43.8(41.0)

ples with constant well-width, but with different barrier compositions. Table II shows the calculated Raman shifts of the SF1 and SF2 signals for donors at the well center and at 10 Å into the barrier as a function of the barrier Mn concentration; a fixed value of $\gamma=0.57$ was used and αN_0 was taken to be 220 meV. The experimental values are given and it is clear that for the $x=0.01$, 0.02, 0.03, and 0.07 samples, the agreement between calculation and experiment is reasonable. There is some uncertainty in the published values of $\bar{x}(x)$ for $x > 0.1$ and this uncertainty is important in the analysis of the data for this series of samples, where x is the parameter that is varied. We therefore performed two sets of calculations taking different estimates for $\bar{x}(x)$, from Refs. 20 and 21 (the values calculated with the latter set of estimates appear in parentheses in Table II). The data of Ref. 20 give the slightly better agreement with our SFR data. For the $x=0.01$ and $x=0.02$ samples, our model predicts that SF1 and SF2 bands will not be sufficiently separated in energy to be experimentally resolved: in both cases only one SFR band is observed, with a Raman shift in agreement with our predictions.

Two other samples which do not form part of the above series are also worth mentioning here. The first is *M387*, which has the *narrowest* quantum wells (15 Å) of all samples investigated and a barrier Mn concentration of 0.09; this sample shows a spin-flip signal at 98.9 cm⁻¹ (at 6 T and 1.6 K) compared to a calculated value for SF1 of about 100 cm⁻¹. The SF2 signal is predicted to be very close to SF1 in this sample (at 105 cm⁻¹) and is not clearly identifiable in the spectra due to the strong PL background at resonance. The second sample is *M213*, which has a relatively wide well (75 Å) and *high* barrier Mn concentration (0.24) and also shows only one resolvable SFR band (at about 8 cm⁻¹). In this latter case, the degree of penetration of the electron wave function into the barrier is negligible, and so only the SF1 signal is predicted to be observable, in agreement with experiment.

The model does not agree so well with the data for the $x=0.12$ sample, *M484*. Only one signal is observed, whose line shape is not well described by either one or two Gaussian bands; we have discussed this point in a previous work,¹⁶ where we showed by consideration of

the resonance energies that the spin-flip signal is still associated with an electron in a quantum well in the material. However, the spin-flip Raman shift is significantly higher than our prediction for SF1 (usually the strongest signal of the two) suggesting either a small degree of interdiffusion, or a reduced degree of Mn spin pairing near the interface, leading to an increased effective Mn concentration in the barrier near the quantum well; we discuss these possibilities in more detail in Sec. VI.

Finally, we note that using the same parameters, and in particular, the same value for γ , we have been able to model successfully the SFR signals observed in asymmetric double quantum-well structures composed of CdTe and Cd_{1-x}Mn_xTe; further details have been presented elsewhere.²⁹

VI. EFFECTS OF INTERDIFFUSION AND OF INTERFACE MAGNETISM

In analyzing our data, we have assumed that the magnetism in the barriers is the same as that in the corresponding bulk Cd_{1-x}Mn_xTe alloy of the same composition. We noted in Sec. III that in the paramagnetic phase, the effects of antiferromagnetic interaction between nearest-neighbor Mn²⁺ ions is such as to decrease the effective number of ions contribution to the paramagnetism and (effectively) to reduce the Mn²⁺ concentration from x to a value \bar{x} (for $x=0.07$, $\bar{x}\approx 0.04$). While such behavior may reasonably be expected to be true for Mn²⁺ ions in the interior of the barrier, it is likely to be modified for those ions at the interface itself, since they will have fewer Mn²⁺ nearest neighbors and, consequently, will give a higher contribution to the paramagnetism.³⁰ The field-induced variation in barrier potential at the interface itself would then be greater than assumed in our model and, in fitting our data, we would have underestimated the conduction-band offset. In our specimens with relatively low barrier concentrations of manganese ($x=0.07$) we do not, however, expect the effect to be important since the wave functions penetrate significantly into the barriers and the electrons interact with Mn²⁺ ions on many monolayers. Furthermore, the studies of Ossau and Kuhn-Heinrich³⁰ show that for

$x < 0.1$, the enhancement of the Mn^{2+} paramagnetism at the interface is small.

Of more serious concern is the possible effect of interdiffusion, since any manganese present in the well itself would give a large contribution to the electron SFR energy. Indeed, one specimen, *M398*, of poor quality and known from x-ray and photoluminescence studies to be significantly interdiffused, shows SFR shifts much greater than predicted by our calculation.

It is difficult to model the effects of interdiffusion without knowledge of the concentration profile, but it is clear that the effects should be more marked in specimens of small well width and high barrier concentrations. A simple approach is to assign an average Mn^{2+} concentration y to the wells, so that the MQW structures are of the form $\text{Cd}_{1-x}\text{Mn}_x\text{Te}/\text{Cd}_{1-y}\text{Mn}_y\text{Te}$ ($x \gg y$). We consider the particular case of *M213*, which has 75-Å wells and a barrier concentration of $x = 0.24$. The observed SFR shift is 8 cm^{-1} (at 6 T), compared with the predicted value of 5 cm^{-1} . The discrepancy may be due to the offset ratio being a function of x , or to reduced spin pairing at the interface, but for the moment we assume (as a worst case) that it is due to interdiffusion. The difference of 3 cm^{-1} between theory and experiment can be accounted for if the average Mn^{2+} concentration in the wells (due to interdiffusion) is $y = 0.001$ (compared with the barrier value $x = 0.24$). If we now assume that the interdiffusion is proportional to the barrier concentrations, the average well concentration in the $x = 0.07$ series would be of order $y = 0.0003$; such a concentration would contribute about 1 cm^{-1} to the Raman shifts of Fig. 9 and would therefore not be important.

VII. THE BAND OFFSET RATIO

Our present results (for $x \approx 0.07$) lead to $\gamma = 0.57 \pm 0.05$ (after correction for strain). Earlier PL and PLE studies of excitonic transitions in $\text{CdTe}/\text{Cd}_{1-x}\text{Mn}_x\text{Te}$ have deduced a wide range of band offsets including a zero valence-band offset,² $\gamma \approx 0.9$ for $x = 0.24$,³ $\gamma \approx 0.6$ for $x = 0.07$,⁴ $\gamma \approx 0.7$, for $x = 0.05$,⁵ $\gamma \leq 0.7$ for $x = 0.07$,⁶ and $\gamma \approx 0.9$ for $x = 0.20$;⁷ it is worth noting that the studies of samples of lower barrier concentration appear to yield lower conduction-band offsets, which are in better agreement with our result. The interpretation of PL and PLE data is complicated by the fact that excitonic binding energies are large and are comparable to the depths of the valence-band potential wells.³¹ The SFR experiments, on the other hand, involve a donor-bound electron which is not part of an exciton, and the interpretation of these experiments is therefore not affected by this problem.

It should be pointed out that since the splitting of the valence band of $\text{Cd}_{1-x}\text{Mn}_x\text{Te}$ by a magnetic field is greater than that of the conduction band and since the valence-band offset is smaller than that of the conduction band, the results of PL and PLE experiments are dominated by the magnitude of the valence-band offset. The effect of interdiffusion would be to reduce the apparent valence-band offset and would thus lead to an *overestimate* of γ , in contrast to our measurements, where man-

ganese interdiffusion into the quantum wells would lead to an *underestimate* of γ .

In summary, for samples with low barrier manganese concentrations, several results derived from PL and PLE and the current electron SFR results suggest a value of $\gamma \approx 0.6$ for the offset ratio in $\text{CdTe}/\text{Cd}_{1-x}\text{Mn}_x\text{Te}$ for $x < 0.10$. This result disagrees with the "common cation" prediction but is close to the prediction of Tersoff.³² The consistent discrepancies in the value of the band offset as determined by different groups appear to be related to the barrier concentration of the specimens used, and it therefore seems likely that γ may be a function of x . It may be possible to resolve this question by further experiments of the type described in the present paper; systematic studies of SFR (and PL and PLE) in samples in which interdiffusion is deliberately induced would also be of help in this context.

VIII. CONCLUSIONS

The most important aspect of this work is the demonstration that spin-flip Raman spectroscopy makes possible the quantitative investigation of the binding of electrons to donors within quantum-well structures. The SFR technique necessitates the use of heterostructures containing dilute magnetic semiconductors, but the model that we have developed in order to explain the present results is of general relevance to nonmagnetic semiconductor heterostructure systems.

The interpretation of spin-flip Raman spectra is less complicated than that of PL and PLE spectra and the line shape and Raman shifts of the signals observed can be modeled within the envelope function approximation, dealing with the conduction-band states alone. We have shown that a relatively simple model is very successful at predicting the structure observed in the spin-flip Raman spectra. The dependence of these spectra on two parameters (well width and barrier concentration) has been studied systematically over two series of specimens and the model reproduces the observed behavior for both series.

When the resonances of the spin-flip Raman signals are to be understood, excitonic effects and the behavior of the valence-band states must be taken into account. Our preliminary results on the resonance behavior of the SFR signals are consistent with the model that we have presented, since a variation in the localization energy of excitons to donors at different positions is to be expected. This would give rise to a difference in the resonance energies of the two Raman signals of the kind that is observed.

Finally, our model for the spin-flip Raman spectra of these quantum-well structures has allowed us to deduce a value for the conduction-band offset and the ratio of this quantity to the total band-gap difference between wells and barriers. Our value is consistent with earlier results obtained by other techniques for samples of similar composition; our results for a large number of samples can be explained satisfactorily without invoking any dependence of this parameter on composition up to Mn concentrations of about 10%. Beyond this concentration, the pos-

sibility remains that the proportion of the band offset in the conduction band increases, and further study is required here. Several problems in the interpretation of magneto-optical studies at higher Mn concentrations have been briefly discussed.

ACKNOWLEDGMENT

The support of the Science and Engineering Research Council of the United Kingdom is gratefully acknowledged.

-
- ¹For reviews of DMS's, see, J. K. Furdyna, *J. Appl. Phys.* **64**, R29 (1989); O. Goede and W. Heimbrodt, *Phys. Status Solidi B* **146**, 9 (1988).
- ²J. Warnock, A. Petrou, R. N. Bicknell, N. C. Giles-Taylor, D. K. Blanks, and J. F. Schetzina, *Phys. Rev. B* **32**, 8116 (1985).
- ³S. K. Chang, A. V. Nurmikko, J. W. Wu, L. A. Kolodziejski, and R. L. Gunshor, *Phys. Rev. B* **37**, 1191 (1988).
- ⁴A. Wasiela, Y. Merle d'Aubigné, J. E. Nicholls, D. E. Ashenford, and B. Lunn, *Solid State Commun.* **76**, 263 (1990).
- ⁵A. Wasiela, P. Peyla, Y. Merle d'Aubigné, J. E. Nicholls, D. E. Ashenford, and B. Lunn, *Semicond. Sci. Technol.* **7**, 571 (1992).
- ⁶S. R. Jackson, J. E. Nicholls, W. E. Hagston, T. J. Gregory, P. Harrison, B. Lunn and D. E. Ashenford, *Superlatt. Microstruct.* **12**, 447 (1992).
- ⁷B. Kuhn-Heinrich, M. Popp, W. Ossau, E. Bangert, A. Waag, and G. Landwehr, *Semicond. Sci. Technol.* **8**, 1239 (1993).
- ⁸For a review of Raman scattering in DMS's, see A. K. Ramdas and S. Rodriguez, in *Semiconductors and Semimetals*, edited by R. K. Willardson and A. C. Beer (Academic, Boston, 1988), Vol. 25.
- ⁹D. L. Peterson, A. Petrou, M. Dutta, A. K. Ramdas, and S. Rodriguez, *Solid State Commun.* **43**, 667 (1982).
- ¹⁰D. L. Peterson, D. U. Bartholomew, U. Debska, A. K. Ramdas, and S. Rodriguez, *Phys. Rev. B* **32**, 323 (1985).
- ¹¹S. I. Gubarev, T. Ruf, and M. Cardona, *Phys. Rev. B* **43**, 14 564 (1991).
- ¹²R. Meyer, M. Hirsch, G. Schaack, A. Waag, and R. N. Bicknell-Tassius, *Superlatt. Microstruct.* **9**, 165 (1991).
- ¹³E.-K. Suh, D. U. Bartholomew, A. K. Ramdas, R. N. Bicknell, R. L. Harper, N. C. Giles, and J. F. Schetzina, *Phys. Rev. B* **36**, 9358 (1987).
- ¹⁴E.-K. Suh, *J. Cryst. Growth* **117**, 890 (1992).
- ¹⁵M. P. Halsall, D. Wolverson, J. J. Davies, D. E. Ashenford, and B. Lunn, *Solid State Commun.* **86**, 15 (1993).
- ¹⁶D. Wolverson, J. J. Davies, S. V. Railson, M. P. Halsall, D. E. Ashenford, and B. Lunn, *J. Cryst. Growth* **138**, 656 (1994).
- ¹⁷D. Wolverson and S. V. Railson, *Meas. Sci. Technol.* **4**, 1080, (1993).
- ¹⁸T. C. Damen, S. P. S. Porto, and B. Tell, *Phys. Rev.* **142**, 570 (1966).
- ¹⁹J. A. Gaj, R. Planel, and G. Fishman, *Solid State Commun.* **29**, 435 (1979).
- ²⁰J. A. Gaj, C. Bodin-Deshayes, P. Peyla, J. Cibert, G. Feuillet, Y. Merle d'Aubigné, R. Romestain, and A. Wasiela, in *Physics of Semiconductors*, edited by Ping Jiang and Hou-Zhi Zheng (World Scientific, Singapore, 1993), p. 923.
- ²¹Y. Shapira, S. Foner, D. H. Ridgley, K. Dwight, and A. Wold, *Phys. Rev. B* **30**, 4021 (1984).
- ²²A. Nakamura, D. Paget, C. Herman, C. Weisbuch, G. Lampel, and B. C. Cavenett, *Solid State Commun.* **30**, 411 (1979).
- ²³M. Hirsch, R. Meyer, and A. Waag, *Phys. Rev. B* **48**, 5217 (1993).
- ²⁴G. Bastard, *Wave Mechanics Applied to Semiconductor Heterostructures* (Editions de Physique, Les Ulis, 1988).
- ²⁵K. Tanaka, M. Nagaoka, and T. Yamabe, *Phys. Rev. B* **28**, 7068 (1983).
- ²⁶R. L. Greene, K. K. Bajaj, and D. E. Phelps, *Phys. Rev. B* **29**, 1807 (1984).
- ²⁷A. Manabe, A. Mitsuishi, and H. Yoshinaga, *Jpn. J. Appl. Phys.* **6**, 593 (1967).
- ²⁸K. K. Kanazawa and F. C. Brown, *Phys. Rev.* **135**, A1757 (1963).
- ²⁹S. V. Railson, D. Wolverson, J. J. Davies, D. E. Ashenford, and B. Lunn, *Superlatt. Microstruct.* **13**, 487 (1993).
- ³⁰W. J. Ossau and B. Kuhn-Heinrich, *Physica B* **184**, 422 (1993).
- ³¹P. Harrison, J. Goodwin, and W. E. Hagston, *Phys. Rev. B* **46**, 12 377 (1992).
- ³²J. Tersoff, *Phys. Rev. Lett.* **56**, 2755 (1986).